ISSN 0021-3640, JETP Letters, 2020, Vol. 112, No. 11, pp. 693–698. © Pleiades Publishing, Inc., 2020.
Russian Text © The Author(s), 2020, published in Pis'ma v Zhurnal Eksperimental'noi i Teoreticheskoi Fiziki, 2020, Vol. 112, No. 11, pp. 730–735.

OPTICS
AND LASER PHYSICS

Efficient Integration of Single-Photon Emitters in Thin InSe Films into Resonance Silicon Waveguides

A. D. Gartman[a], M. K. Kroichuk[a], A. S. Shorokhov[a], and A. A. Fedyanin[a, *]

[a] *Faculty of Physics, Moscow State University, Moscow, 119991 Russia*

**e-mail: fedyanin@nanolab.phys.msu.ru*

Received September 1, 2020; revised October 26, 2020; accepted October 28, 2020

A concept of the optimal design of a silicon waveguide based on optically coupled Mie-resonant nanoantennas for efficient inputting of light from point emitters associated with excitons localized at defects in a thin InSe film is proposed. Numerical calculations demonstrate that the efficiency of coupling between a dipole emitter and a resonant silicon waveguide is four orders of magnitude greater than that for a conventional ridge waveguide.

DOI: 10.1134/S002136402023006X

Among the various platforms for performing quantum computations, integrated photonics has a special place owing to good potential for scalability, the availability of well-elaborated fabrication technologies, and the possibility of using existing facilities for the manufacturing of such devices [1]. The implementation of novel efficient single-photon light emitters on an integrated chip is one of the priority tasks for the further development of this field [2]. The practical usefulness of such emitters is often determined by their compatibility with modern semiconductor technologies, as well as by the requirement of a high efficiency, which is determined by the brightness and the indistinguishability of individual photons.

A variety of solid-state single-photon emitters currently exist [3]. The most common ones include color centers in crystals, i.e., fluorescent point defects, of which the most studied are the nitrogen–vacancy and silicon–vacancy defects (NV and SiV centers, respectively) in diamond [4, 5], carbon nanotubes, and quantum dots based on III–V semiconductors like GaAs/InAs [6, 7]. Another type of single-photon emitters becoming popular in recent years is based on two-dimensional materials [8], for example, dichalcogenides (S, Se, and Te) of transition metals (Mo or W) and boron nitride [9]. Layered group-III–VI chalcogenides, such as gallium and indium selenides, were extensively investigated in [10, 11], where the optical selection rules and the possibility of the existence of so-called gray exciton transitions, whose dipole moment can feature pronounced anisotropic properties, were described in detail. Recently, it was also demonstrated that gray exciton transitions exist in ultrathin chalcogenides films with the number of layers from 1 to 10 [12]. The orientation of point dipole emitters in this case will be determined by the electronic properties and selection rules of the host semiconductor [13]. Quantum-confinement effects allow controlling the band gap in such compounds from infrared to ultraviolet by changing the number of layers in chalcogenide films from a multilayer structure to a monolayer [14]. This makes thin films of chalcogenides an attractive object for further research and implementation of single-photon emitters for integrated quantum optics [15, 16]. It is worth noting that traditional solid-state emitters are usually embedded in bulk materials with a high refractive index, which limits the efficiency of photon emission and the capacity for integration. In contrast, the two-dimensional geometry of thin films makes it possible to simplify their integration with photonic circuits and to significantly increase the yield of the useful signal [17].

Typically, the efficiency of an integrated emitter can be raised in two ways: (i) by increasing the quantum yield owing to the Purcell effect [18] or (ii) by increasing the efficiency of coupling the emitted light to a waveguide structure on a chip. A high quantum yield can be achieved by using plasmon resonators, characterized by small modal volumes, or dielectric resonators, where very high Q factors can be attained [19]. However, the Purcell effect in plasmonic structures depends significantly on the position of the emitter, and a high absorption coefficient in metals leads to high losses. This makes dielectric resonators more attractive. Furthermore, they are more frequently based on materials that are compatible with modern CMOS technology. In order to effectively input radiation from a single-photon emitter directly into an integrated circuit, strong optical coupling between the emitter and the waveguide system on the chip should

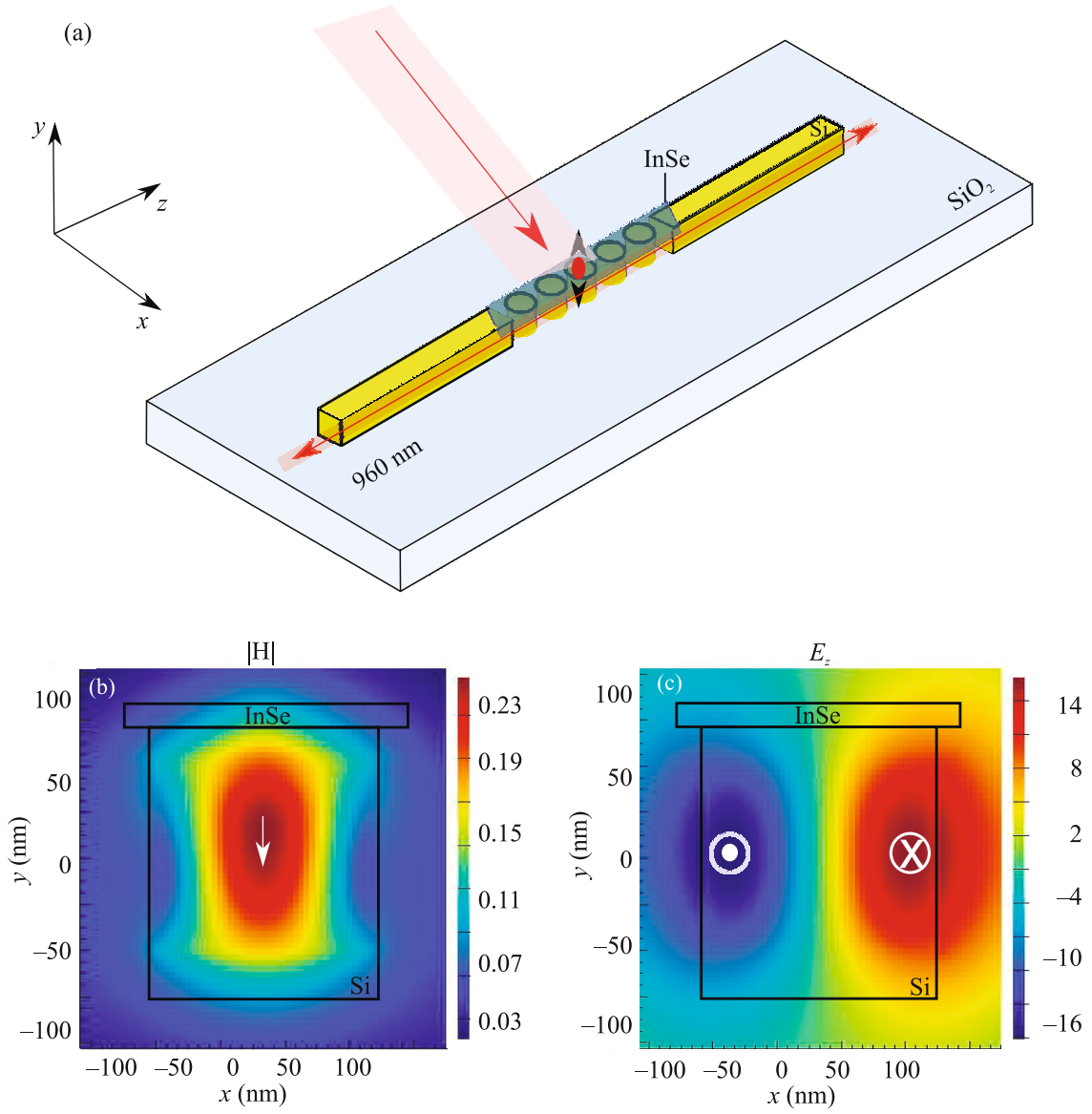

Fig. 1. (Color online) (a) Layout of the silicon waveguide system under study arranged on a substrate. The middle part of the waveguide is formed by a chain of silicon nanocavities covered with a 10-nm InSe film. (b, c) Distributions of the (b) magnetic and (c) electric fields in the cross section of the central silicon disk with a diameter of 260 nm under the conditions of the magnetic-dipole Mie resonance excited by a point emitter located in the InSe film.

exist. This can be achieved, in particular, in a resonant waveguide system consisting of nanoantennas made of a material with a high refractive index [20]. The excitation of electric- and magnetic-dipole Mie resonances in such nanoantennas [21] makes it possible to effectively control both the linear and nonlinear optical responses of such structures [22, 23]. It was shown that, by arranging such nanoantennas into one-dimensional chains, one can ensure efficient propagation of radiation owing to near-field optical coupling between them when a magnetic-dipole Mie resonance is excited in individual particles [24]. Such waveguide systems have a number of advantages, which allow developing new functional devices on an optical chip based on these systems [25].

Here, we suggest a concept of the effective integration of single-photon emitters in thin InSe films with resonant waveguides of this type based on silicon nanoparticles. As discussed above, InSe is chosen because it features gray excitons, which can be excited out-of-plane. This is important for efficient coupling with the waveguide system. The layout of the structure under study is shown in Fig. 1a. Point dipole emitters in the thin InSe film are associated with localized exci-

ton states formed owing to the presence of defects in the film [26]. It should be noted that such an emitter can be excited both optically and electrically [27]. The calculations reported below disregard the Purcell effect and imply the existence of a dipole emitter with a given intensity immediately in the thin InSe film at a given light wavelength. According to [12], the absorption spectrum of a thin (~10 nm) InSe film at a temperature of 10 K features an exciton transition at about 1.29 eV, which corresponds to a wavelength of 960 nm. The choice of these films is fundamentally justified because absorption in silicon in this spectral range is low. Further analysis was carried out for the case of a dipole emitter at this wavelength and a 10-nm InSe film. This simplification makes it possible to focus on the study of the efficiency of coupling between the dipole emitter and the magnetic optical mode of Mie resonance silicon nanodisks.

Using the Lumerical FDTD software package, we carried out finite-difference time-domain numerical simulation of a system consisting of a ridge silicon waveguide with a height of 160 nm and a width of 140 nm whose middle part is formed by a chain of disk-shaped nanocavities with a height of $h = 160$ nm and a period of $s = 50$ nm covered on top with a 10-nm InSe film that contains a point dipole emitting at a wavelength of 960 nm. The numerically calculated distributions of the electric and magnetic fields in the cross section of the central silicon disk with a diameter of 260 nm (see Figs. 1b, 1c) demonstrate the appearance of a magnetic-dipole Mie resonance in the nanoantennas upon their excitation by the point emitter located in the InSe film. A layout with typical parameters used in the calculations is shown in the top part of Fig. 2a for the situation where the system is immersed in an isotropic medium with a refractive index of $n = 1.45$. The main part of Fig. 2b shows the dependence of the transmission coefficient for this configuration of the resonant system with and without a thin InSe film on top (black and red lines, respectively) on the diameter of the silicon nanodisks. Here, the transmission coefficient is defined as the ratio $T = I_{in}/I_{out}$ of the intensities of radiation at the input and output of the waveguide system. In both cases, the highest transmission is attained when the diameter of the nanocavities is 140 nm and equals $T = 0.96$ and 0.93, respectively. Similar calculations were carried out for the situation where the waveguide system is placed on a semi-infinite SiO_2 substrate (see Fig. 2c). The highest transmission in the case of a waveguide covered with an InSe film equals $T = 0.98$ and is attained when the diameter of the silicon nanodisks is $d = 250$ nm. Without an InSe film, the highest transmission is $T = 0.76$ and is attained for $d = 260$ nm. The high transmission attained in both configurations (with the resonant waveguide system in a homogeneous medium and on a SiO_2 substrate) means that efficient optical coupling occurs between the nanoantennas of the waveguide system when the magnetic-dipole resonance is excited in them. This efficient coupling is achieved owing to the optimum design of the system.

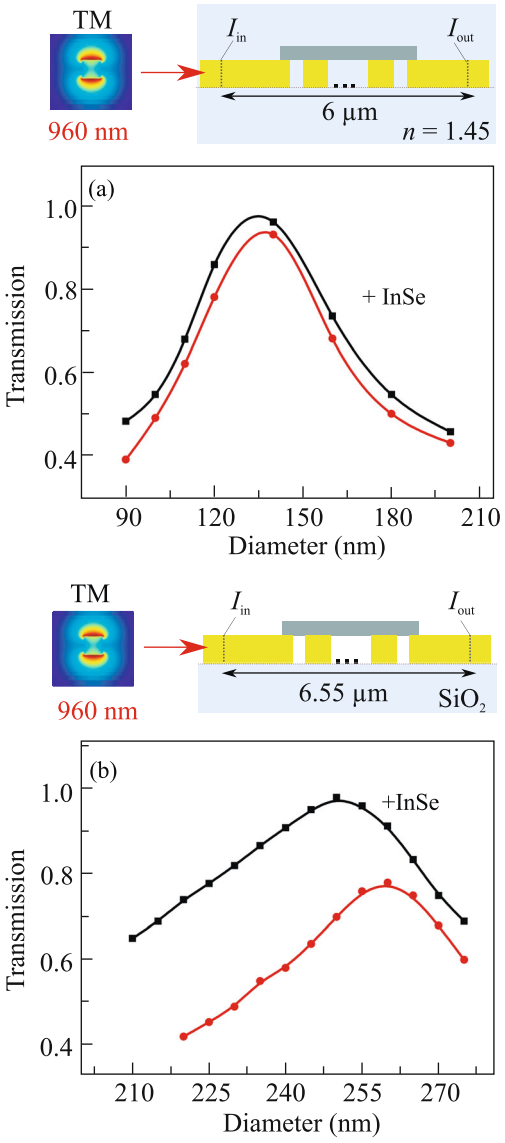

Fig. 2. (Color online) Transmission coefficient of a resonant waveguide system versus the diameter of silicon nanodisks for (a) the structure in an isotropic environment with a refractive index of 1.45 and (b) the structure on a SiO_2 substrate. The black and red lines correspond to the structures with and without a 10-nm InSe film covering the disks, respectively. The layout of the analyzed structure is shown above each of the plots.

To analyze the efficiency of collecting radiation emitted by point dipoles associated with excitons localized at defects in the thin InSe film, we compared the intensity I_{res} of light at the exit of the resonant waveguide structure with the intensity I_{ref} at the exit of a continuous ridge waveguide with the same height

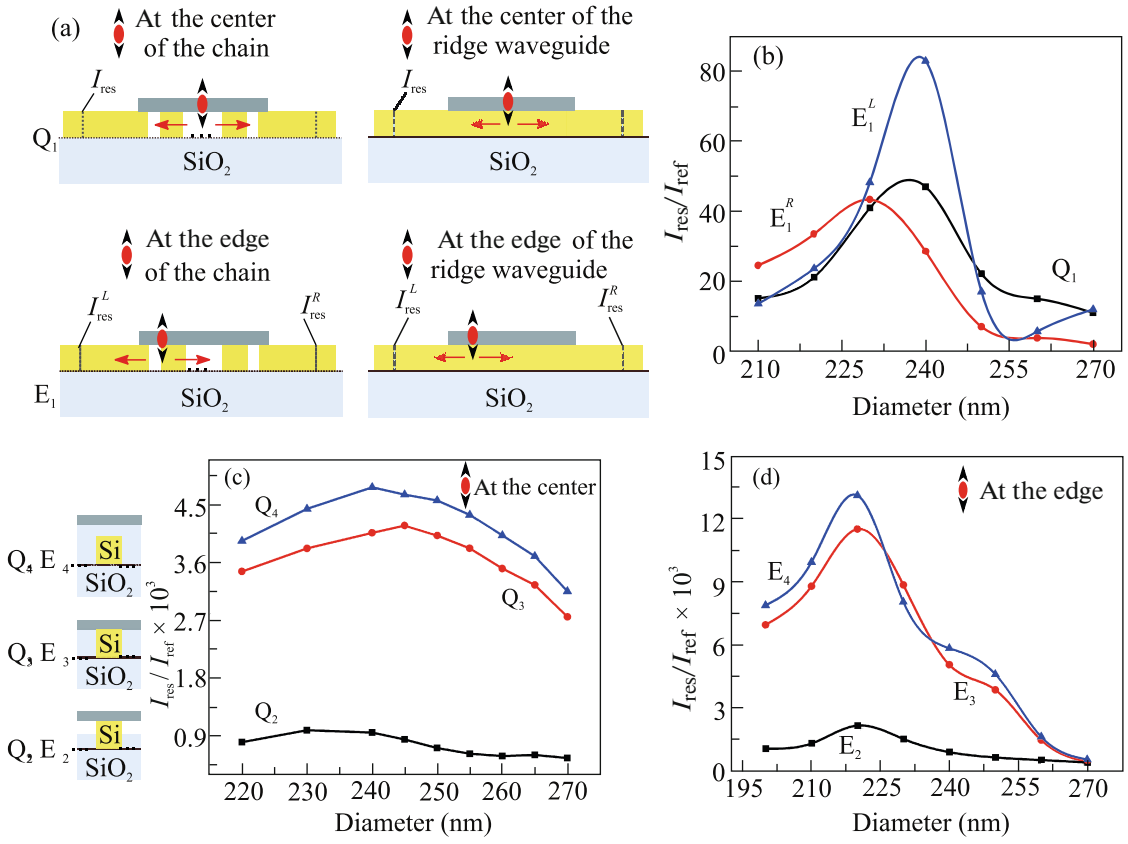

Fig. 3. (Color online) (a) Layouts of resonant waveguide structures with different locations of the emitter in the InSe film. Space between the nanodisks is empty in samples Q_1 and E_1, filled with silicon dioxide to a height of $h/2$ in samples Q_2 and E_2, filled with silicon dioxide to a height of h in samples Q_3 and E_3, and filled with silicon dioxide to 10 nm above the height of the nanodisks h in samples Q_4 and E_4. (b–d) Relative efficiency of the coupling of electromagnetic radiation emitted by a point dipole in the InSe film to the waveguide structure versus the diameter of silicon nanodisks: (b) the defect is located at the center and the edge of the structure in configurations Q_1 and E_1, respectively; (c) the defect is located at the center of the structure in configurations Q_2, Q_3, and Q_4, respectively; and (d) the defect is located at the center of the structure in configurations E_2, E_3, and E_4, respectively.

and width. The efficiency is characterized by the ratio $A_{\text{eff}} = I_{\text{res}}/I_{\text{ref}}$. We considered several configurations of the samples differing from each other in two respects: the location of the dipole emitter in the thin film relative to the waveguide system (at the center or at the edge of the waveguide system in samples of types Q and E, respectively) and the filling of space between the silicon nanodisks with a dielectric material (the same as the substrate material). This is shown schematically in Fig. 3a: space between the nanodisks is empty in samples Q_1 and E_1, filled with silicon dioxide to a height of $h/2$ in samples Q_2 and E_2, filled with silicon dioxide to a height of h in samples Q_3 and E_3, and filled with silicon dioxide to 10 nm above the height of the nanodisks in samples Q_4 and E_4.

We considered the cases of a dipole emitter located both at the center and at the edge of the resonance disk system (Fig. 3a). The relative efficiency of the coupling of electromagnetic energy from the point emitter to the waveguide channel for configurations Q_1 and E_1 is shown in Fig. 3b; here, E_1^L and E_1^R correspond to radiation coupling to the waveguide sections closer and farther from the emitter, respectively. The highest value of A_{eff} in resonant systems with disk diameters d between 210 and 270 nm is obtained for $d = 240$ nm. We note that an increase in the coupling efficiency A_{eff} attained for the resonant system of silicon nanodisks in comparison to a continuous ridge waveguide may be as large as a factor of 80 or 45 in the cases where the dipole emitter is located at the edge (sample Q_1) or at the center (sample E_1) of the nanodisk array, respectively.

Figure 3c shows the dependences of A_{eff} for a point dipole located at the center of the structure (samples of type Q) on the diameter of silicon nanodisks in the range of 220 to 270 nm for different fillings of space

between the nanodisks with a dielectric medium whose refractive index equals that of the substrate (fused silica (SiO_2) was chosen for the calculations). When the silicon nanocavities are immersed in such a medium, a dynamic increase in the efficiency of energy transfer from the point emitter to the resonant waveguide takes place. The maxima of the dependences $A_{eff}(d)$ shift to smaller values of d.

Similar dependences presented in Fig. 3d were calculated for the case of a point dipole located at the edge of the silicon nanodisk chain (samples of type E). The highest efficiency A_{eff} is attained for $d = 220$ nm and equals 13.6×10^3 and 11.9×10^3 for configurations E_3 and E_4, respectively, and 2.8×10^3 for configuration E_2. Therefore, it is possible to maximize the coupling of radiation emitted by the point dipole by optimizing the geometry of nanocavities and varying the refractive index of the medium filling space between them. We mention that filling the space between nanodisks with a material identical to that of the substrate makes the investigated system closer to the model case of an isotropic dielectric medium considered above.

It is noteworthy that here we consider only effects related to an increase in the efficiency of the optical coupling of radiation emitted by a point dipole in an InSe thin film to the waveguide structure owing to the optimal selection of the geometric parameters of the nanoantennas forming the structure. The Purcell effect, which affects the quantum yield of the emitter, was disregarded (the model considered an emitter with a given quantum yield). Meanwhile, by optimizing the geometry of the waveguide system, it would be possible, apart from an increase in the efficiency of optical coupling between the emitter and the waveguide, to obtain an increase in the quantum yield of the emitter. In addition, replacing silicon with a material having a lower absorption coefficient, such as silicon nitride, may be promising [28, 29].

In summary, we have carried out a numerical simulation of resonant semiconductor structures where radiation from a point emitter in a thin InSe film can be efficiently coupled to a waveguide system with Mie resonance silicon nanodisks. We have shown that the use of resonant nanostructures makes it possible to increase the efficiency of optical coupling between the waveguide and the emitter in such a film by four orders of magnitude compared to a conventional ridge waveguide owing to the excitation of the magnetic-dipole resonance in nanoparticles built into the waveguide. These results can be used to create efficient nonclassical light emitters on an optical chip for integrated quantum photonics.

ACKNOWLEDGMENTS

We are grateful to T.V. Shubina for useful comments and advice.

FUNDING

This study was supported by the Russian Foundation for Basic Research, project nos. 19-32-90223 (simulation of the optical coupling between the quantum emitter and the waveguide) and 18-29-20097 (numerical optimization of the transmission of the resonant waveguide). Part of the study was supported by the Quantum Technology Center, Moscow State University.

REFERENCES

1. J. Wang, F. Sciarrino, A. Laing, and M. G. Thompson, Nat. Photon. **14**, 273 (2020).
2. M. D. Eisamana, J. Fan, A. Migdall, and S. V. Polyakov, Rev. Sci. Instrum. **82**, 071101 (2011).
3. I. Aharonovich, D. Englund, and M. Toth, Nat. Photon. **10**, 631 (2016).
4. A. Krasnok, A. Maloshtan, D. Chigrin, Y. Kivshar, and P. Belov, Laser Photon. Rev. **9**, 385 (2015).
5. F. Lenzini, N. Gruhler, N. Walter, and W. H. P. Pernice, Adv. Quantum Technol. **1**, 1800061 (2018).
6. C. Dietrich, A. Fiore, M. Thompson, and S. Hofling, Laser Photon. Rev. **10**, 6 (2016).
7. S. Hepp, M. Jetter, S. Portalupi, and P. Michler, Adv. Quantum Technol. **2**, 1900020 (2019).
8. X. Liu and M. Hersam, Nat. Rev. Mater. **4**, 669 (2019).
9. K. Novoselov, A. Mishchenko, A. Carvalho, and A. Castro Neto, Science (Washington, DC, U. S.) **353**, 6298 (2016).
10. M. Kuroda, I. Munakata, and Y. Nishina, Solid State Commun. **33**, 687 (1980).
11. P. Gomes da Costa, R. G. Dandrea, R. F. Wallis, and M. Balkanski, Phys. Rev. **48**, 14135 (1993).
12. M. Brotons-Gisbert, R. Proux, R. Picard, D. Andres-Penares, A. Branny, and B. D. Gerardot, Nat. Commun. **10**, 3913 (2019).
13. T. Shubina, W. Desrat, M. Moret, A. Tiberj, O. Briot, V. Davydov, and A. Platonov, Nat. Commun. **10**, 3479 (2019).
14. H. Chen, M. Palummo, D. Sangalli, and M. Bernardi, Nano Lett. **18**, 3839 (2018).
15. S. Tamalampudi, Y. Lu, R. Kumar, and R. Sankar, Nano Lett. **14**, 2800 (2014).
16. C. Chakraborty, N. Vamivakas, and D. Englund, Nanophotonics **8**, 2017 (2019).
17. S. Ren, Q. Tan, and J. Zhang, J. Semicond. **40**, 7 (2019).
18. P. Yao, V. S. C. Manga Rao, and S. Hughes, Laser Photon. Rev. **4**, 499 (2010).
19. M. Pelton, Nat. Photon. **9**, 427 (2015).
20. O. Sergaeva, I. Volkov, and R. Savelev, Nanosyst.: Phys. Chem. Math. **10**, 266 (2019).
21. A. Kuznetsov, A. Miroshnichenko, M. Brongersma, Y. Kivshar, and B. Luk'yanchuk, Science (Washington, DC, U. S.) **18**, 354 (2016).

22. M. K. Kroychuk, A. S. Shorokhov, D. F. Yagudin, D. A. Shilkin, D. A. Smirnova, M. R. Shcherbakov, and A. A. Fedyanin, Nano Lett. **5**, 3471 (2020).
23. E. V. Melik-Gaykazyan, K. L. Koshelev, J. H. Choi, S. S. Kruk, A. A. Fedyanin, and Y. S. Kivshar, JETP Lett. **109**, 131 (2019).
24. R. Bakker, Y. Yu, and A. Kuznetsov, Nano Lett. **17**, 3458 (2017).
25. P. Cheben, R. Halir, and H. Atwater, Nature (London, U.K.) **560**, 565 (2018).
26. G. Mudd, M. Molas, X. Chen, V. Zolyomi, K. Nogajewski, Z. R. Kudrynskyi, Z. D. Kovalyuk, G. Yusa, O. Makarovsky, and L. Eaves, Sci. Rep. **6**, 39619 (2016).
27. C. Chakraborty, L. Kinnischtzke, K. Goodfellow, R. Beam, and A. Vamivakas, Nat. Nanotechnol. **10**, 507 (2015).
28. F. Peyskens, C. Chakraborty, M. Muneeb, D. Thourhout, and D. Englund, Nat. Commun. **10**, 4435 (2019).
29. W. Elshaari, W. Pernicz, K. Srinivasan, O. Benson, and V. Zwiller, Nat. Photon. **12**, 285 (2020).

Translated by M. Skorikov